Limnol. Oceanogr., 56(3), 2011, 857–866

doi:10.4319/lo.2011.56.3.0857

Spatial variability of emergence, splash, surge, and submergence in wave-exposed rocky-shore ecosystems

K. A. S. Mislan,[a,1,*] Carol A. Blanchette,[b] Bernardo R. Broitman,[c,d] and Libe Washburn[b]

[a] Department of Biological Sciences, University of South Carolina, Columbia, South Carolina
[b] Marine Science Institute, University of California, Santa Barbara, California
[c] Centro de Estudios Avanzados en Zonas Áridas, Facultad de Ciencias del Mar, Universidad Católica del Norte, Coquimbo, Chile
[d] Center for Advanced Studies in Ecology and Biodiversity, Pontificia Universidad Católica de Chile, Santiago, Chile

Abstract

To distinguish the intertidal states of emergence, splash, surge, and submergence and record their relative durations, we deployed a water-level logger paired with a temperature logger in the mid-intertidal zone at each of 10 wave-exposed sites during the summer in the northeast Pacific. Relative durations of intertidal states were different among the different sites, even at sites close together. Splash was temporally variable, being recorded by the loggers on 50% or fewer days at most sites. Daily surge durations tended to be longer at sites in northern and central California compared with sites in Oregon and Washington. Return times to surge and submergence showed the opposite trend with longer return times in Oregon and Washington compared with California. We estimated the effect of interannual changes in tides on intertidal states by applying the logger data to tidal predictions and comparing duration and return time over the 18.6-yr tidal epoch. Over long time periods, compared with the logger deployments, daily durations of surge increased, return times to the surge state became more uniform, and return times to submergence lengthened.

Organisms inhabiting wave-exposed rocky intertidal shorelines are alternately exposed to marine and terrestrial conditions following the rhythm of the tidal cycle (Lewis 1964). Superimposed on this more or less predictable variation in exposure is a much more unpredictable regime of exposure to wet and dry conditions created by the splash and surge of wave action (Thomas 1986). Splash occurs as water droplets caused by waves spray over the intertidal surface, moistening it while it is still aerially exposed. Splash is highly variable both spatially and temporally, and the amount of splash is largely determined by instantaneous wave and wind conditions and local topography. Surge is more consistent than splash in areas with habitual waves and can be defined as the time period when there is high frequency variation on the scale of minutes between submergence and emergence states as waves run up on the intertidal bench. Intertidal organisms have adapted to the wave-exposed intertidal environment by exploiting favorable conditions and enduring unfavorable conditions. Because most intertidal organisms evolved from marine origins, most critical biological functions (feeding, reproduction, etc.) occur when the organisms are underwater (Newell 1970).

Quantifying the allocation of time among the intertidal states can help determine the mechanisms driving the distribution and abundance of intertidal organisms (Stephenson and Stephenson 1949; Lewis 1964). One method divided the shore by tidal benchmarks, mean higher high water (MHHW), mean lower high water (MLHW), mean higher low water (MHLW), and mean lower low water (MLLW), approximating the relative amounts of emersion vs. submersion over long time periods (Colman 1933; Doty 1946; Hartnoll and Hawkins 1982). This approach has only been partially successful for determining ecological mechanisms because there was no way to quantify the intermediate phases of surge and splash with benchmarks (Doty 1946). More recently, the concept of effective shore level (ESL) was used to measure emersion time more precisely. ESL was determined with the use of rapid temperature changes recorded by in situ temperature loggers to identify the timing of the first splash (Harley and Helmuth 2003; Gilman et al. 2006). The tidal elevation at this moment signified the ESL and the end of emersion time. The difference between ESL and the actual still tidal level was thus assumed to represent the amount of wave run-up, but it was not able to distinguish between splash, surge, and submergence.

Among the intertidal states, surge, in particular, has been difficult to quantify directly with instruments (Thomas 1986; Burrows et al. 2008). Direct measurements of the surge state would increase understanding of critical biological functions and physiological performance of intertidal organisms. High algal productivity in wave-exposed areas has been linked to the increased exposure of fronds to light by movement from wave action during the surge state (Wing and Patterson 1993), as well as protection from desiccation because of constant spray and splash from waves (Nielsen et al. 2006). During the surge stage, invertebrates are able to start consuming oxygen because most are able to respire in air as well as water, as long as humidity remains high, and may be able to excrete acid by-products resulting from anaerobic metabolism when covered by water (Newell 1970). Some invertebrates also may be able to feed and metabolize during this time. For example, during the surge state under high-flow conditions, suspension feeders such as barnacles may not actively pump or move filtering appendages but can passively

* Corresponding author: kas.mislan@gmail.com

[1] Present address: Atmospheric and Oceanic Sciences Program, Princeton University, Princeton, New Jersey

obtain food from the rushing water (Crisp and Southward 1961; Trager et al. 1990; Wildish and Kristmanson 1997). The surge state can also be a dangerous time for organisms inhabiting wave-exposed habitats during stormy conditions. High wave action can damage or kill by dislodging all or parts of invertebrates and macroalgae from the rocks (Denny 1985; Denny et al. 1985). Many mobile marine invertebrates are inhibited from feeding during this period of time because they must adhere to the substrate (Denny and Blanchette 2000). Thus, the surge environmental stage has benefits and hazards for intertidal organisms.

We directly quantified the relative duration of emergence, splash, surge, and submergence by deploying a temperature logger paired with a water level logger in the mid-intertidal zones of 10 wave-exposed rocky intertidal sites along the Pacific coast of North America (Fig. 1). We examined metrics of these intertidal states that are physiologically relevant to intertidal organisms: durations of intertidal states and their return times. Duration defines the amount of time spent in a particular intertidal state, and characteristics of duration could be drivers of physiological adaptation in intertidal organisms. Return times to surge or submergence define how long intertidal organisms are exposed to aerial conditions and the potentially stressful effects of desiccation, high or low temperature, and wave action. For organisms that depend on the submergence state, return times to submergence could be critical. In addition, we observed the effect of interannual variations in tides by estimating the durations and return times that occur during the course of the 18.6-yr tidal epoch by using tidal predictions and the transitions between intertidal states (Denny and Paine 1998; Mislan et al. 2009).

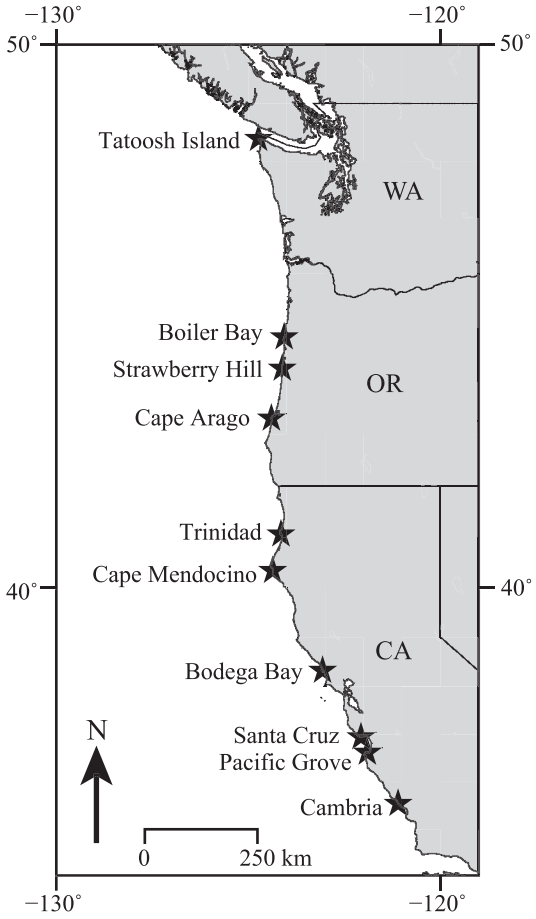

Fig. 1. Map of field site locations in the northeast Pacific. The abbreviations for the states are WA, Washington; OR, Oregon; CA, California.

Methods

Logger deployments—Water level loggers (Onset Hobo® 13-Foot Depth Data Loggers) and temperature loggers (Onset TidbiT Temperature Data Loggers) were deployed in the mid-intertidal zone within 40 cm of the median tide level at 10 sites between Washington and California (Fig. 1). Tidal height was approximate and selected so loggers would be exposed to emergence, splash, surge, and submergence conditions daily. Before deployment, water level loggers were encased in a perforated polyvinyl chloride (PVC) pipe with end caps to protect the loggers. The PVC pipe was anchored to the rocky substrate with stainless steel straps. Adjacent to the PVC pipe, a temperature logger embedded in epoxy was attached with Z-Spar Splash Zone Epoxy, with the thermistor oriented seaward. Temperature and water level loggers recorded at 2-min intervals for 30 d at each site, with sampling frequency limited by the water level logger memory. After water level loggers were retrieved from field sites, pressure data were converted into water levels according to the hydrostatic pressure equation,

$$h = \frac{P_{\log} - P_{\text{air}}}{\rho g}, \quad (1)$$

where h is the height of the water column (m), $P_{\log}$ and P_{air} are logger pressure and atmospheric pressure, respectively (Pa), ρ is the density of seawater (kg m^{-3}); and g is acceleration due to gravity (m s^{-2}). Atmospheric pressure data, P_{air}, were obtained from different sources depending on the site (Table 1). For density, ρ, we used a value of 1021 kg m^{-3}, which is a representative density of open-ocean water at the surface (Pickard and Emery 1990). The value 9.81 m s^{-2} was used for gravity, g.

After pressure data were converted to water level, a minor temperature correction was applied. Loggers reached high temperatures during aerial exposure on low tides, causing slightly inaccurate ($<$ 10 cm) water level records during those periods. The correction was determined experimentally by placing a pressure logger and sampling temperature and pressure at 1-s intervals under a halogen lamp for 110 min. The temperature of the water level logger under the halogen lamp increased from 10.26°C to 48.69°C. A second pressure logger, also sampling at 1-s intervals, was placed in the same room but away from the lamp during the same time period to control for pressure changes not associated with temperature. The data were converted to water level (m) according to the hydrostatic pressure equation; $P_{\log}$ data came from the logger under the lamp, and P_{air} data came from the control logger. Water level

Table 1. Data resources used for the calculations in this study. TTIW1, KARYACHA2, and CARO3 are names identifying specific weather stations. Mean daily tidal amplitude was calculated in meters for each site during the deployment period.

Sites (N to S)	Lat. (°)	Long. (°)	Air pressure	XTide station	Mean daily tidal amplitudes (m)	Wave height and period
Tatoosh Island	48.39	−124.74	NOAA NDBC C-MAN TTIW1	Tatoosh Island, Cape Flattery, Strait of Juan de Fuca, Washington	2.39	NOAA buoy 46087 (2004–2006)
Boiler Bay	44.83	−124.06	Hadfield weather station	Depoe Bay, Oregon	2.53	NOAA buoy 46050 (1997–2006)
Strawberry Hill	44.25	−124.11	Wunderground KARYACHA2	Siuslaw River, Entrance	2.31	NOAA buoy 46050 (1997–2006)
Cape Arago	43.31	−124.40	NOAA NDBC C-MAN CARO3	Charleston, Coos Bay, Oregon	2.31	NOAA buoy 46015 (2002–2006)
Trinidad	41.06	−124.15	NCDC–Arcata airport	Trinidad Harbor, California	2.13	NOAA buoy 46022 (1997–2006)
Cape Mendocino	40.35	−124.36	Wunderground–Petrolia	Humboldt Bay Entrance, California	1.97	NOAA buoy 46213 (2004–2006)
Bodega Bay	38.32	−123.07	NOAA NDBC buoy 46013	Bodega Harbor Entrance, California	1.75	NOAA buoy 46013 (1997–2006)
Santa Cruz	36.95	−122.06	NOAA NDBC buoy 46042	Santa Cruz, Monterey Bay, California	1.65	NOAA buoy 46042 (1997–2006)
Pacific Grove	36.62	−121.90	NOAA NDBC buoy 46092	Monterey, Monterey Harbor, California	1.77	NOAA buoy 46042 (1997–2006)
Cambria	35.54	−121.09	NOAA NDBC buoy 46028	San Simeon, California	1.72	NOAA buoy 46028 (1997–2006)

Lat, latitude; Long, longitude; NOAA, National Oceanographic and Atmospheric Administration; NDBC, National Data Buoy Center; NCDC, National Climatic Data Center; C-MAN, Coastal–Marine Automated Network.

values were regressed against logger temperature, and a quadratic regression was fitted to the data ($R^2 = 0.99$, $n = 6640$) so that the temperature of the logger could be used to determine the water level correction for high temperatures,

$$h_{\text{corr}} = 0.00005T^2 - 0.0007T + 0.0115, \quad (2)$$

where h_{corr} is the amount subtracted from the converted water level data (m), and T is water level logger temperature (°C). After correction, water level logger data were correctly analyzed as zero when emerged even when exposed to high air temperatures. The water level loggers record temperature as well as pressure during data collection, so T is always available, and this temperature is representative of the temperature inside the perforated PVC tube that protects the water level logger in the intertidal zone.

Comparison of wave run-up—Loggers were deployed for a 30-d period at each site in 2007 (Table 2). All of the deployments were during May to August, so loggers collected data during summertime wave regimes. The geographically widespread deployment of loggers limited their temporal extent to ca. 30 d and made it necessary to determine whether wave run-up during the deployment period was relevant over the entire summer season. Using the equations and parameters from Schoch et al. (2006), we estimated wave run-up because run-up has an important influence on the timing of intertidal states, especially surge, in the wave-exposed intertidal. Hourly Significant Wave Height and Dominant Wave Period, which are required for determining wave run-up, were obtained from National Oceanic and Atmospheric Administration (NOAA) buoys located nearest each site (Table 1).

Hourly wave run-up (m) with data from the NOAA buoys was calculated for the period of individual logger deployments in 2007. Means and variances of wave run-up during logger deployment were then compared with simulated hourly wave run-up created by subsampling from the 10 previous years of buoy data, 1997–2006. Some buoys were not deployed for 10 yr, so in these cases, fewer years were used (Table 1: Tatoosh Island, Cape Arago, Cape Mendocino). We simulated run-up by randomly selecting 24-h periods with replacement, created 1000 run-up datasets, and compared them to buoy wave run-up during logger deployments. Using a two-sample t-test and a variance ratio test, we compared means and variances of these 1000 replicate tests, respectively. The run-up datasets had serial dependence because they were time series, so an effective sample size and an adjusted variance for data with serial dependence were used in the comparisons (Wilks 2006). In this analysis, we wanted to determine whether the entire summer season had similar wave run-up to the logger deployment period, so we were interested in the nonsignificant statistical results ($p > 0.05$). A high proportion of nonsignificant values meant that the wave run-up during logger deployment (30 d) appeared to be representative of wave run-up during a season (90+ d). Simulated run-up

Table 2. Calculations based on predicted tides for the transition points between intertidal states at the logger locations. The logger level is the still-water shore level of the logger deployment location. Percent days with splash is the number of days with splash divided by the number of days with a 1°C temperature drop. Levels are the height of the predicted tide during the transition point.

Sites (N to S)	Deployment dates in 2007	Logger level intcpt.±error (m above tidal datum)	% days with splash	Em.–spl. level (m; mean±SD)	Spl.–sur. level (m; mean±SD)	Sur.–sub. level (m; mean±SD)
Tatoosh Island	29 Jul–28 Aug	1.69±0.0023 (r^2=0.80)	73	1.15±0.24 (n=19)	1.48±0.14 (n=120)	1.80±0.09 (n=106)
Boiler Bay	18 Jul–17 Aug	1.28±0.0015 (r^2=0.95)	33	1.08±0.16 (n=12)	1.08±0.15 (n=98)	1.31±0.10 (n=122)
Strawberry Hill	17 Jul–18 Aug	1.24±0.0019 (r^2=0.89)	5	1.15±0.09 (n=19)	0.98±0.39 (n=92)	1.03±0.44 (n=104)
Cape Arago	19 Jul–18 Aug	1.28±0.0028 (r^2=0.71)	38	0.95±0.22 (n=8)	0.83±0.39 (n=100)	1.19±0.36 (n=142)
Trinidad	18 May–17 Jun	1.31±0.0022 (r^2=0.85)	35	1.04±0.11 (n=14)	1.02±0.33 (n=128)	1.29±0.48 (n=121)
Cape Mendocino	19 May–18 Jun	1.29±0.0023 (r^2=0.68)	40	0.80±0.15 (n=5)	0.96±0.24 (n=106)	1.50±0.25 (n=98)
Bodega Bay	5 May–4 Jun	1.18±0.0021 (r^2=0.47)	50	0.52±0.13 (n=14)	0.69±0.22 (n=90)	1.25±0.22 (n=179)
Santa Cruz	4 May–3 Jun	0.97±0.0021 (r^2=0.75)	39	0.49±0.09 (n=18)	0.31±0.30 (n=58)	0.69±0.40 (n=147)
Pacific Grove	5 Jun–5 Jul	1.09±0.0029 (r^2=0.62)	50	0.58±0.23 (n=12)	0.57±0.40 (n=79)	1.35±0.18 (n=76)
Cambria	11 May–10 Jun	0.82±0.0017 (r^2=0.89)	82	0.29±0.08 (n=11)	0.64±0.09 (n=81)	1.04±0.08 (n=126)

Em.–spl., emergence–splash; Spl.–sur., splash–surge; Sur.–sub., surge–submergence; intcpt., y-intercept.

datasets were subsampled from all months (January to December) and summer months (April to September). Summer months were considered to be June to August at the northernmost sites: Tatoosh Island, Boiler Bay, Strawberry Hill, and Cape Arago.

Logger data analysis—Splash was calculated by applying the effective shore level method to the temperature logger data; Gilman et al. (2006) provide an in-depth description of this method. Briefly, the temperature logger records a sudden drop in temperature during the transition between the emergence and splash intertidal states because the ocean water is frequently much cooler than the temperature logger at the end of a low tide on sunny days. With the use of this method, direct measurements of splash could only be determined for a rising tide. The water level logger data were used to quantify more information about the intertidal states. Emergence or splash occurred when the water level loggers recorded a water level of 0 m for 30 min. Surge values, as recorded by the water level loggers, fluctuated between water levels of 0 and $>$ 0 m. When water level loggers consistently recorded values $>$ 0 m for 30 min, as shown in Fig. 2 state D, it was considered to be in the submergence state. Emergence and splash were distinguished by classifying the intertidal state as ''splash'' when temperature drops occurred after a low tide and the water level logger recorded 0 m.

Tidal epoch analyses—Logger data were compared with tidal predictions obtained from XTide (Flater 2006) to determine transitions between emergence, splash, surge, and submergence as controlled by the tide. Tidal heights at the transition times are referred to as ''levels'' and are the heights of the predicted tides during the changes in intertidal state. The emergence–splash level, splash–surge level, and surge–submergence level were determined for each transition by comparing the transition times recorded by the loggers with the predicted tidal elevation at the transition time. XTide stations used to generate the predicted tides are listed in Table 1. Tidal elevations at transition times were then averaged within each category—emergence–splash level, splash–surge level, and surge–submergence level—for the entire logger deployment period. Next, we applied the levels (emergence–splash level, splash–surge level, and surge–submergence level) derived from the logger data to tidal predictions over 18.6 yr, the length of the tidal epoch (Schureman 1941; Kaye and Stuckey 1973; Denny and Paine 1998). We analyzed tidal predictions from the summer months, which had wave run-ups similar to those during the 30 d of logger deployment (Table 3).

Still water shore level—The still water shore level of the logger deployment location was also calculated with the water level data. To approximate the still water condition, wave effects were removed from the water level logger data by taking a running median of the data with a five-point filter equivalent to an 8-min period. Then data corresponding to emergence times were removed (i.e., water levels = 0 m), and the remaining running median values were

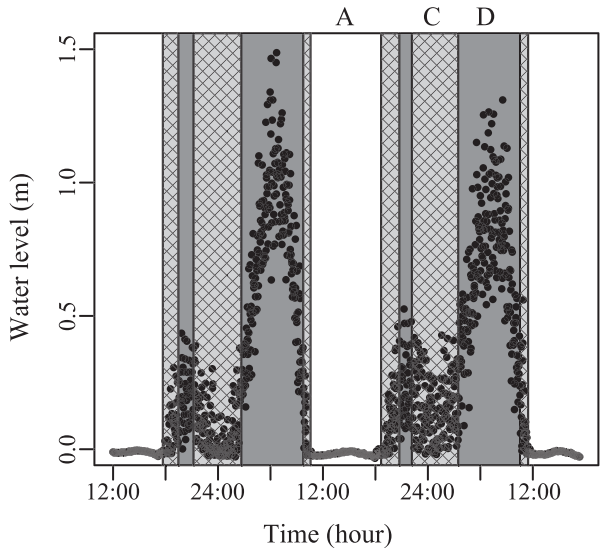

Fig. 2. Data from the water level logger deployed at Cambria, California, depicting the differences among recordings of environmental states of emergence, surge, and submergence. A, white backgrounds, are the periods of emergence or splash; C, gray-patterned backgrounds, are the surge periods; D, gray backgrounds, are the periods of submergence.

regressed against tidal predictions from the nearest tide station (Table 1). It was necessary to remove the emergence times because only the time periods when water level loggers were covered by the tide were relevant for this analysis. A linear (least squares) fit between predicted and observed water levels was determined with the running median, in which the *y*-intercept of the prediction estimated the still water shore level of the logger.

Analyses of intertidal states—Duration was represented as the modal number of observations in each intertidal state. Kernel density smoothing with a bi-weight smoothing kernel was used to provide an objective estimate of bin size and alignment when determining the modal duration (Wilks 2006). Return times to the surge and submergence states were determined and illustrated in the form of a violin plot, which combines a box plot with a kernel-smoothed histogram, revealing both the range and distribution of return times (Hintze and Nelson 1998).

Results

The proportion of nonsignificant results of the two-sample *t*-test and the variance ratio test indicated that wave run-up during logger deployment (logger run-up) was similar to summer wave run-up, but not similar to annual wave run-up (Table 3). The mean and variance of the logger run-up were similar to summer wave run-up in 56.4–100% and 42.9–93.8% of simulation comparisons, respectively. For Tatoosh Island, Boiler Bay, Strawberry Hill, and Cape Arago, summer wave run-up during April through September was not similar to logger run-up. Therefore, we adjusted the summer months to June through August for these sites, thereby greatly increasing the proportions of similar results. The summer months, as listed in Table 3, were the only time periods considered in the tidal epoch analyses.

The relative durations of splash, surge, and submergence could be important for the timing and duration of intertidal organism physiological activity, so they will be considered first. The method to measure splash was dependent on a $> 1^{\circ}$C difference in logger and ocean temperature during low tide, a condition requiring that low tide be during the day and the weather be sunny. Therefore, splash was measured as the number of days with splash (1°C temperature drop and water level = 0 m) divided by the total days with a 1°C temperature drop (Table 2). Tatoosh Island, Bodega Bay, Pacific Grove, and Cambria had 50% or more of days with splash, whereas Strawberry Hill had only 5% of days with splash. Figure 3 shows the relative

Table 3. Results from seasonal comparisons of wave run-up between the logger deployment periods and simulations. The mean and SD columns are the means and standard deviations (m) of wave run-up in simulation sampling pools. The *n* column gives the number of sample points for that locale. *See* Table 1 for the date ranges of *n*.

	Annual (January–December)					Summer*				
			Wave run-up (m)					Wave run-up (m)		
	$p(t$ ns)	$p(F$ ns)	Mean	SD	*n*	$p(t$ ns)	$p(F$ ns)	Mean	SD	*n*
Tatoosh Island	0.002	0.270	1.728	0.783	18,974	0.564	0.929	1.223	0.406	5683
Boiler Bay	0.000	0.029	2.184	1.057	73,354	0.911	0.881	1.42	0.450	19,486
Strawberry Hill	0.002	0.075	2.184	1.057	73,354	0.901	0.826	1.42	0.450	19,486
Cape Arago	0.000	0.082	2.187	0.997	31,280	0.645	0.867	1.482	0.447	9042
Trinidad	0.276	0.667	2.205	0.981	77,597	0.995	0.938	1.700	0.643	37,742
Cape Mendocino	0.332	0.757	2.282	0.894	17,421	1.000	0.889	1.825	0.606	7274
Bodega Bay	0.289	0.690	2.068	0.831	73,559	0.975	0.907	1.726	0.588	38,362
Santa Cruz	0.366	0.652	2.046	0.798	77,401	0.993	0.804	1.683	0.523	38,233
Pacific Grove	0.902	0.950	2.046	0.798	77,401	1.000	0.429	1.683	0.523	38,233
Cambria	0.428	0.476	2.158	0.798	71,438	0.989	0.871	1.845	1.565	37,117

$p(t$ ns), the proportion of nonsignificant ($p>0.05$) two-sample *t*-tests out of 1000 comparisons; $p(F$ ns), the proportion of nonsignificant ($p>0.05$) variance ratio tests out of 1000 comparisons.

* Summer is June–August for Tatoosh Island, Boiler Bay, Strawberry Hill, and Cape Arago; it is April–September for all other locales.

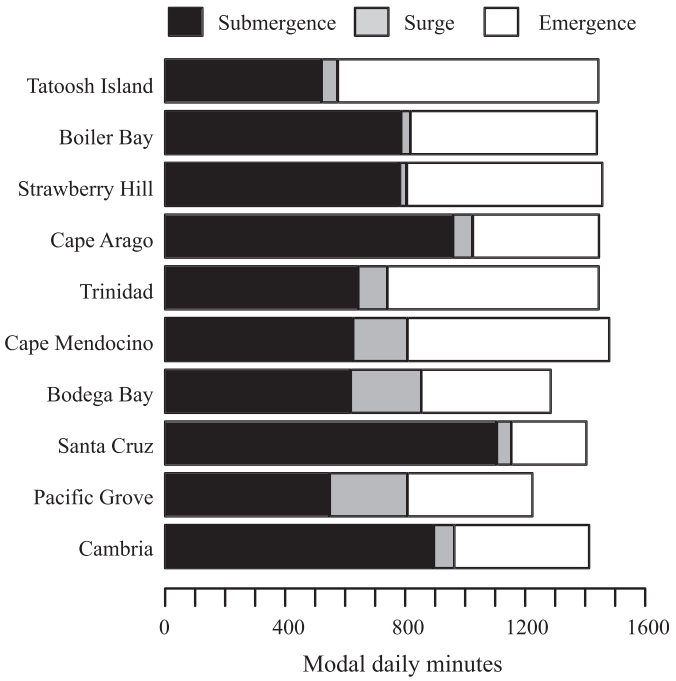

Fig. 3. Relative durations of emergence, surge, and submergence as recorded by the loggers during the deployment period. Splash was temporally variable, so modal daily minutes were close to zero for all the sites. The intertidal states did not necessarily sum to 1440 min (i.e., 24 h) per day in the analysis because modes were used.

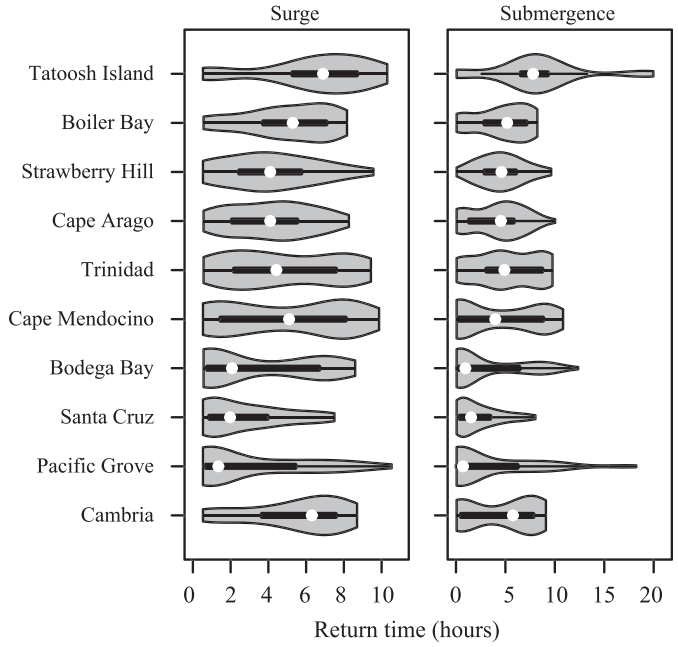

Fig. 4. Return times to the surge and submergence states as recorded by the loggers during the deployment period. The "violin" shapes are the kernel density–smoothed representations of the frequency distributions. The white circles are the medians. The bold lines extending horizontally from the circles are the 25th and 75th percentiles of the distributions. The thin lines extending horizontally from the bold lines are 1.5 times the interquartile range (IQR).

differences between daily emergence, surge, and submergence as recorded by the water level loggers. Although there are 1440 min d^{-1}, the intertidal states did not necessarily sum to 1440 min d^{-1} in the analysis because modes were used. Splash was not included in this analysis because it was measured too infrequently, and the modal value was close to 0 (i.e., < 3 min). Bodega Bay and Pacific Grove had the most minutes of surge per day, which was 235 and 259 min, respectively; Boiler Bay and Strawberry Hill had the fewest minutes of surge per day, which was 31 and 23 min, respectively (Fig. 3). Santa Cruz had the most minutes per day of submergence, 1106 min, when compared with the other sites. Pacific Grove had the fewest minutes per day of submergence, 550 min, which was half the Santa Cruz submergence time. No overall trend with latitude was observed in the relative modal durations of emergence, surge, and submergence.

Return times to surge represent the amount of time that organisms are continuously exposed to the terrestrial environment. The median return times to surge recorded by the loggers ranged from 1.4 h in Pacific Grove to 6.9 h on Tatoosh Island. The majority of sites, including Boiler Bay, Strawberry Hill, Cape Arago, Trinidad, and Cape Mendocino, had median return times to surge that were 4–5 h (Fig. 4). The maximum return times to surge are another important characteristic to consider. The maximum return times to surge ranged from 7.5 h at Terrace Point to 10.3 h on Tatoosh Island.

Return times to submergence are the time intervals dividing the periods when organisms are constantly underwater. The median return times to submergence recorded by the loggers were similar to the median return times to surge. Boiler Bay, Strawberry Hill, Cape Arago, Trinidad, and Cape Mendocino had median return times to submergence of 4–5 h (Fig. 4). Bodega Bay, Santa Cruz, and Pacific Grove had the shortest median return times to submergence, which were < 2 h. Tatoosh Island had the longest median return time to submergence of 7.8 h. Figure 4 shows that Tatoosh Island and Pacific Grove had the longest maximum return times to submergence recorded by the loggers, which were 20 and 18.2 h, respectively. Except for Bodega Bay, which had a maximum return time to submergence of 12.4 h, the rest of the sites had maxima that were < 11 h. In general, median return times decreased from north to south. Cambria, the southernmost site, was an exception to this trend, having median return times to surge of 6.3 h and to submergence of 5.8 h.

The 18.6-yr tidal epoch analyses determined the potential effect of interannual changes in tides on relative durations and return times during the summer. In Fig. 5, the relative duration of splash was only determined for Tatoosh Island, Cape Mendocino, Bodega Bay, and Cambria because these are the only sites for which there was a difference in the emergence–splash level and the splash–surge level (Table 2). Tatoosh Island had 192 modal daily minutes of splash, the greatest relative duration among the sites. Pacific Grove had the most modal daily surge, 742 min, and Strawberry Hill had the least modal daily surge, 31 min, during the tidal epoch. Submergence

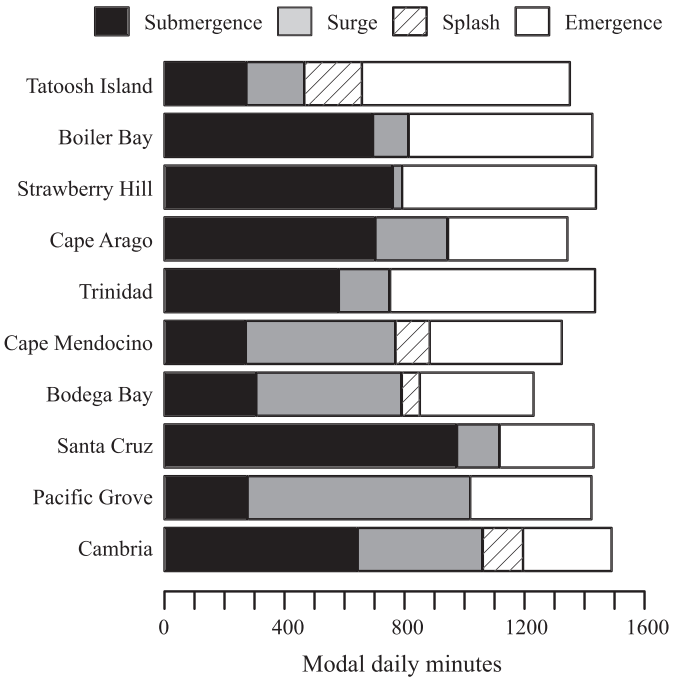

Fig. 5. Relative durations of emergence, splash, surge, and submergence during an 18.6-yr tidal epoch. Tidal predictions were obtained from XTide. The intertidal states did not necessarily sum to 1440 min (i.e., 24 h) per day in the analysis because modes were used.

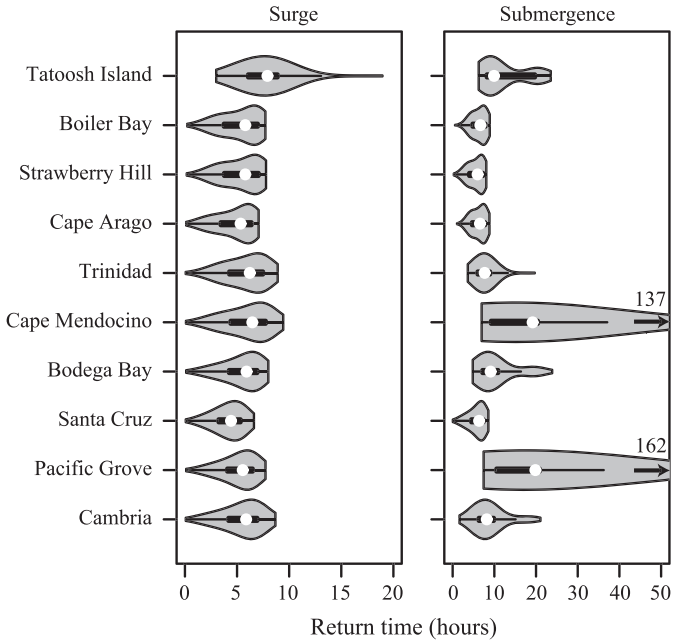

Fig. 6. Return times to surge and submergence during an 18.6-yr tidal epoch. The "violin" shapes are the kernel density–smoothed representations of the frequency distributions. The white circles are the medians. The bold lines extending horizontally from the circles are the 25th and 75th percentiles of the distributions. The thin lines extending horizontally from the bold lines are 1.5 times the interquartile range (IQR).

ranged from 277 min in Pacific Grove to 975 min in Santa Cruz.

Over a tidal epoch, the return times to surge had similar distributions across the sites (Fig. 6). The median return times to surge ranged from 4.4 h in Santa Cruz to 7.9 h on Tatoosh Island, and the maximum return times to surge ranged from 6.6 h in Santa Cruz to 19 h on Tatoosh Island. Excluding Tatoosh Island, the maximum return times to surge for the sites were 8 ± 0.8 h (mean ± SD). The median return times to submergence during the tidal epoch ranged from 6 h in Strawberry Hill to 19.8 h in Pacific Grove (Fig. 6). Maximum return times to submergence had a trimodal distribution, with Boiler Bay, Strawberry Hill, Cape Arago, and Santa Cruz having an average maxima of 8.6 ± 0.38 h (mean ± SD); Tatoosh Island, Trinidad, Bodega Bay, and Cambria having an average maxima of 22 ± 2 h (mean ± SD); and Cape Mendocino and Pacific Grove having an average maxima of 149.3 ± 17.5 h (mean ± SD).

Discussion

This study partitions the intertidal environment into conditions of emergence, splash, surge, and submergence. Splash was recorded on 50% or fewer days at most of the sites, likely because of the temporal variability in wave conditions (Table 2). Organisms living in the vicinity of the logger deployment locations in Cambria and Tatoosh Island were influenced by more consistent splash, 82% and 73% of days, respectively, than the other sites. Organisms at these locations might benefit the most from splash cooling on days when weather conditions could otherwise lead to harmfully high body temperatures (Harley and Helmuth 2003). Strawberry Hill had the lowest percentage of days with splash because the logger was deployed in a relatively more protected location than at the other sites. Unfortunately, splash could not be recorded on days without solar radiation during low tide by this method. This study focused on summer conditions, which is the best time to estimate splash with the ESL method because solar radiation is high and storms are rare.

Surge was recorded at all study sites, as was expected, because all sites were specifically chosen to be in wave-exposed locations (Fig. 3). Northern sites tended to have a very limited period of daily surge time recorded by the loggers. A possible reason for this pattern is the greater tidal amplitudes at northern sites, which means water levels increase and decrease more quickly and thus pass more quickly through the intermediate surge stage. However, this latitudinal pattern might cease in winter when northern sites are exposed to more extreme wave conditions (J. C. Allan and P. D. Komar unpubl.). Figure 3 also shows a pattern in which sites with relatively shorter durations of surge had relatively greater durations of submergence on a daily basis during the summer. The mechanism driving this pattern is not apparent. However, sites located in close geographic proximity, such as Bodega Bay, Santa Cruz, and Pacific Grove, demonstrate that patterns in surge and submergence are site specific and not necessarily related to latitudinal patterns of tides and waves. Pacific Grove and Bodega Bay had the most minutes per day of surge, but

among the fewest submergence minutes. Conversely, Santa Cruz had the most submergence minutes per day. Assuming that organisms are differentially adapted to surge and submergence states, organisms that benefit from long periods of surge time are expected to be more abundant at surge-dominated sites, and organisms that benefit from long periods of submergence time are expected to be more abundant at submergence-dominated sites. We suggest this hypothesis for future investigation.

The median return times to surge and submergence tended to decrease with decreasing latitude, a trend that might also be related to the reduction in tidal amplitude that occurs from north, $\sim$ 2.53 m, to south, $\sim$ 1.72 m, along this coastline (Fig. 4; Table 1). Cambria, the site located farthest south, was an anomaly, with the median return times closest to those for Boiler Bay, one of the sites located farthest north. Helmuth et al. (2006) found that mussels living in the rocky intertidal in Boiler Bay and Cambria experience greater thermal variability than intervening sites, which might be connected to the similar return times to surge. The maximum return times to surge and submergence likely pose the greatest risks for desiccation stress and therefore could be important for organisms living in the rocky intertidal. Pacific Grove had the lowest median return times to surge and submergence and the highest maximum return times. Therefore, organisms living at this site were experiencing consistently short return times, occasionally punctuated by unusually long return times during logger deployment. In contrast, Santa Cruz, the closest site geographically, had the shortest maximum return times. Overall, patterns in median return times appeared to have a latitudinal trend, whereas the maximum return times seemed to be uniquely related to a site.

Waves are responsible for short-term variation, but tides control the rise and fall of water in the intertidal habitat over longer time scales. Historically well measured, tides vary on an 18.6-yr cycle called the tidal epoch and can be predicted with harmonic constants calculated from long-term observations (Cartwright 1999). By combining tidal predictions with the tidal levels associated with intertidal states (Table 2), it is possible to model the tidal influence on durations and return times over the tidal epoch. Figure 5 shows that interannual changes in tides during the epoch will more than double the modal minutes of surge observed during the logger deployments (Fig. 3). The tidal epoch simulations also clarified the dominant role of surge in the daily cycle of Cape Mendocino, Bodega Bay, and Pacific Grove over longer time scales (Fig. 5). Interannual increases in daily surge were usually matched by interannual decreases in daily submergence. Splash was measured at four sites where the splash–surge level was higher than the emergence–splash level (Table 2). Except for Pacific Grove, these were also the sites that had the highest percentages of days with recorded splash. In Pacific Grove, the splash–surge level approximately equaled the emergence–splash level, and 50% of the days had recorded splash. The standard deviations of both emergence–splash level and splash–surge level in Pacific Grove were the highest measured in this study. Thus, the timings of these transitions at this site were relatively more variable, which could explain the equality of the emergence–splash level and the splash–surge level. The variability in the timing of the transitions was likely related to the topography and orientation of the site and not unusual wave characteristics during the logger deployment because, as the results in Table 3 show, wave run-up appeared to be typical for the summer season in Pacific Grove.

Latitudinal gradients in return times to surge and submergence, clearly apparent in the logger data, were not evident in the median return times to surge when the tidal epoch was considered (Fig. 6). For the return times to surge, a uniformity across sites appeared in the medians and maxima, so the short-term differences recorded during the logger deployments might not be important for intertidal organisms over longer time scales. Tatoosh Island, the most northern site, had a longer median return time and a much more extreme maximum return time to surge. However, the wave run-up analysis found that wave run-up during the logger deployment on Tatoosh Island was $\sim$ 56% representative of the typical wave run-up during the summer season (Table 3). If the wave run-up during the logger deployment was more representative, the median and maximum return times to surge during the tidal epoch might resemble the other sites.

In sharp contrast to return times to surge, return times to submergence became much less uniform across sites when the tidal epoch was considered. Organisms living in the vicinity of the logger deployment locations would experience a return time to submergence of < 24 h at most sites. However, at two sites, Cape Mendocino and Pacific Grove, return times to the submergence state might last for 5–6 d at occasional points during the tidal epoch. Extremely long return times could be detrimental and possibly lethal to organisms dependent on the submergence state (Underwood and Denley 1984). One explanation for the extreme differences among sites in the return times to submergence might be the small differences in the shore level of deployment locations: locations closer to MHHW are more likely to display extreme return times. The loggers were deployed as close to the median shore level as possible, but the shore level could only be approximated at the time of deployments. However, further analysis of still water shore level difference from MHHW indicated that Cape Mendocino (0.61 m) and Pacific Grove (0.51 m) were deployed > 0.50 m below MHHW and were similar to other sites, including Trinidad (0.69 m), Bodega Bay (0.52 m), and Santa Cruz (0.63 m). Alternatively, the duration of the surge state might explain the extremely long return times to submergence. Figure 5 supports this explanation, with Cape Mendocino and Pacific Grove having the longest modal daily minutes of surge. This emphasizes that surge is an important physical characteristic to measure, and in situ measurements of surge, with water-level loggers, for example, will be crucial for a more comprehensive understanding of species abundance and distribution in the intertidal environment.

Differences in duration and return time of surge and submergence among sites might drive variation in intertidal community assemblages. Wave fetch, which can be used as

a wave exposure index—a measurement related to magnitude and frequency of surge—has proved to be an important predictor of intertidal communities (Thomas 1986; Burrows et al. 2008). In the northeast Pacific, several recent studies on the distribution and abundance of intertidal organisms have spanned the same coastline and included many of the same sites (Connolly and Roughgarden 1998; Schoch et al. 2006; Blanchette et al. 2008). Findings from these studies indicate many common taxa across these sites, although abundance varies site-to-site. Furthermore, changes in diversity in the mid-zones were not significantly related to the latitudinal gradient from north to south, even though many environmental variables are significantly related to the gradient (Schoch et al. 2006). Therefore site-to-site differences in surge and submergence time might better explain variability in abundances and diversity. The ecological significance of surge and submergence time will need to be further clarified with the use of field-based experiments during logger deployments.

Acknowledgments

We thank B. Helmuth for providing loggers for this study and C. Pfister, T. Wootten, R. Paine, Makah Tribal Council, Bodega Marine Reserve, J. Sones, E. Sanford, and P. Raimondi for help accessing field sites. We appreciated field site assistance from M. George, J. Bram, P. Martone, R. Martone, L. Miller, M. Noble, E. Richmond, and A. Salomon. M. Denny, D. Wethey, and S. Woodin contributed helpful insights. This manuscript was greatly improved by comments from B. Helmuth, V. Lakshmi, D. Wethey, S. Woodin, and two anonymous reviewers.

Funding sources included a National Aeronautics and Space Administration (NASA) Earth Systems Science Fellowship, an Elsie Tabor Travel Grant, NASA grant NNX07AF20G, and National Oceanic and Atmospheric Administration (NOAA) Ecofore grant NA04NOS4780264.

References

Blanchette, C. A., C. M. Miner, P. A. Raimondi, D. Lohse, K. E. K. Heady, and B. R. Broitman. 2008. Biogeographic patterns of rocky intertidal communities along the Pacific coast of North America. J. Biogeogr. **35:** 1593–1607, doi:10.1111/j.1365-2699.2008.01913.x

Burrows, M. T., R. Harvey, and L. Robb. 2008. Wave exposure indices from digital coastlines and the prediction of rocky shore community structure. Mar. Ecol. Prog. Ser. **353:** 1–12, doi:10.3354/meps07284

Cartwright, D. E. 1999. Tides: A scientific history. Cambridge Univ. Press.

Colman, J. 1933. The nature of intertidal zonation of plants and animals. J. Mar. Biol. Assoc. UK **18:** 435–476, doi:10.1017/S0025315400043794

Connolly, S. R., and J. Roughgarden. 1998. A latitudinal gradient in northeast Pacific intertidal community structure: Evidence for an oceanographically based synthesis of marine community theory. Am. Nat. **151:** 311–326, doi:10.1086/286121

Crisp, D. J., and A. J. Southward. 1961. Different types of cirral activity of barnacles. Philos. Trans. R. Soc. Lond. B Biol. Sci. **243:** 271–307, doi:10.1098/rstb.1961.0003

Denny, M. W. 1985. Wave forces on intertidal organisms: A case study. Limnol. Oceanogr. **30:** 1171–1187, doi:10.4319/lo.1985.30.6.1171

———, and C. A. Blanchette. 2000. Hydrodynamics, shell shape, behavior, and survivorship in the owl limpet *Lottia gigantea*. J. Exp. Biol. **203:** 2623–2639.

———, T. L. Daniel, and M. A. R. Koehl. 1985. Mechanical limits to size in wave-swept organisms. Ecol. Monogr. **55:** 69–102, doi:10.2307/1942526

———, and R. T. Paine. 1998. Celestial mechanics, sea-level changes, and intertidal ecology. Biol. Bull. **194:** 108–115, doi:10.2307/1543040

Doty, M. S. 1946. Critical tide factors that are correlated with the vertical distribution of marine algae and other organisms along the Pacific Coast. Ecology **27:** 315–328, doi:10.2307/1933542

Flater, D. XTide. [Internet]. [accessed 2009 February 15]. Available from http://www.flaterco.com/xtide/

Gilman, S. E., C. D. G. Harley, D. C. Strickland, O. Vanderstraeten, M. J. O'Donnell, and B. Helmuth. 2006. Evaluation of effective shore level as a method of characterizing intertidal wave exposure regimes. Limnol. Oceanogr.: Methods **4:** 448–457.

Harley, C. D. G., and B. S. T. Helmuth. 2003. Local- and regional-scale effects of wave exposure, thermal stress, and absolute versus effective shore level on patterns of intertidal zonation. Limnol. Oceanogr. **48:** 1498–1508, doi:10.4319/lo.2003.48.4.1498

Hartnoll, R. G., and S. J. Hawkins. 1982. The emersion curve in semidiurnal tidal regimes. Estuar. Coast. Shelf Sci. **15:** 365–371, doi:10.1016/0272-7714(82)90047-6

Helmuth, B., and others. 2006. Mosaic patterns of thermal stress in the rocky intertidal zone: Implications for climate change. Ecol. Monogr. **76:** 461–479, doi:10.1890/0012-9615(2006)076[0461:MPOTSI]2.0.CO;2

Hintze, J. L., and R. D. Nelson. 1998. Violin plots: A box plot–density trace synergism. Am. Stat. **52:** 181–184, doi:10.2307/2685478

Kaye, C. A., and G. W. Stuckey. 1973. Nodal tidal cycle of 18.6 Yr.: Its importance in sea-level curves of the east coast of the United States and its value in explaining long-term sea-level changes. Geology **1:** 141–144, doi:10.1130/0091-7613(1973)1<141:NTCOYI>2.0.CO;2

Lewis, J. R. 1964. The ecology of rocky shores. English Univ. Press.

Mislan, K. A. S., D. S. Wethey, and B. Helmuth. 2009. When to worry about the weather: Role of tidal cycle in determining patterns of risk in intertidal systems. Glob. Change Biol. **15:** 3056–3065, doi:10.1111/j.1365-2486.2009.01936.x

Newell, R. C. 1970. Biology of intertidal animals. American Elsevier.

Nielsen, K. J., C. A. Blanchette, B. A. Menge, and J. Lubchenco. 2006. Physiological snapshots reflect ecological performance of the sea palm, *Postelsia palmaeformis* (Phaeophyceae) across intertidal elevation and exposure gradients. J. Phycol. **42:** 548–559, doi:10.1111/j.1529-8817.2006.00223.x

Pickard, G. L., and W. J. Emery. 1990. Descriptive physical oceanography. Butterworth-Heinemann.

Schoch, G. C., B. A. Menge, G. Allison, M. Kavanaugh, S. A. Thompson, and S. A. Wood. 2006. Fifteen degrees of separation: Latitudinal gradients of rocky intertidal biota along the California Current. Limnol. Oceanogr. **51:** 2564–2585, doi:10.4319/lo.2006.51.6.2564

Schureman, P. 1941. Manual of harmonic analysis and prediction of tides. Special Publication No. 98. U.S. Coast and Geodectic Survey, U.S. Government Printing Office.

Stephenson, T. A., and A. Stephenson. 1949. The universal features of zonation between tide-marks on rocky coasts. J. Ecol. **37:** 289–305, doi:10.2307/2256610

Thomas, M. L. H. 1986. A physically derived exposure index for marine shorelines. Ophelia **25:** 1–13.

Trager, G. C., J.-S. Hwang, and J. R. Strickler. 1990. Barnacle suspension feeding in variable flow. Mar. Biol. **105:** 117–127, doi:10.1007/BF01344277

Underwood, A. J., and E. J. Denley. 1984. Paradigms, explanations, and generalizations in models for the structure of intertidal communities on rocky shores, p. 151–180. *In* D. R. Strong, D. Simberloff, L. G. Abele, and A. B. Thistle [eds.], Ecological communities: Conceptual issues and the evidence. Princeton Univ. Press.

Wildish, D., and D. Kristmanson. 1997. Benthic suspension feeders in flow. Cambridge Univ. Press.

Wilks, D. S. 2006. Statistical methods in the atmospheric sciences, 2nd ed. Academic.

Wing, S. R., and M. R. Patterson. 1993. Effects of wave-induced lightflecks in the intertidal zone on photosynthesis in the macroalgae *Postelsia palmaeformis* and *Hedophyllum sessile* (Phaeophyceae). Mar. Biol. **116:** 519–525, doi:10.1007/BF00350069

Associate editor: Chris Rehmann

Received: 03 April 2010
Accepted: 29 December 2010
Amended: 23 January 2011